Challenges to Estimating Tree Height via LiDAR in Closed-Canopy Forests: A Parable from Western Oregon

Demetrios Gatziolis, Jeremy S. Fried, and Vicente S. Monleon

Abstract: We examine the accuracy of tree height estimates obtained via light detection and ranging (LiDAR) in a temperate rainforest characterized by complex terrain, steep slopes, and high canopy cover. The evaluation was based on precise top and base locations for >1,000 trees in 45 plots distributed across three forest types, a dense network of ground elevation recordings obtained with survey grade equipment, and LiDAR data from high return density acquisitions at leaf-on and leaf-off conditions. Overall, LiDAR error exceeded 10% of tree height for 60% of the trees and 43% of the plots at leaf-on and 55% of the trees and 38% of the plots at leaf-off. Total error was decomposed into contributions from errors in the estimates of tree top height, ground elevation model, and tree lean, and the relationships between those errors and stand- and site-level variables were explored. The magnitude of tree height error was much higher than those documented in other studies. These findings, coupled with observations that indicate suboptimal performance of standard algorithms for data preprocessing, suggest that obtaining accurate estimates of tree height via LiDAR in conditions similar to those in the US Pacific Northwest may require substantial investments in laser analysis techniques research and reevaluation of laser data acquisition specifications. FOR. SCI. 56(2):139–155.

Keywords: airborne laser scanning, Pacific Northwest, terrain modeling, tree leaning, calibration

TREE HEIGHT IS a critical attribute assessed in most forest inventories (McCombs et al. 2003). It is used to estimate volume, biomass, and carbon stores of individual trees and to compute site index and various indices of forest structure (e.g., late successional status and canopy fuel characteristics). Traditionally, tree height is assessed via labor-intensive and comparatively costly field mensuration techniques or a combination of field measurements and modeling. Forest managers and inventory specialists have long sought alternative, more economical approaches to obtain tree heights that meet established accuracy standards (Aldred and Hall 1975). Remote sensing technologies have been regarded as perhaps the most promising direction to pursue (Johnson 1958, Kovats 1997).

To a much greater degree than aerial photography and other forms of optical remote sensing, light detection and ranging (LiDAR), an evolving remote sensing technology sometimes referred to as airborne laser scanning, can penetrate forest canopies, making it particularly well-suited to describing the vertical profile of forests (Lim et al. 2003). Since the late 1990s, laser scanning has become an important component of forest management and inventory operations in many countries (Hyyppä et al. 2003, Nilsson et al. 2003, Wulder 2003). It has been successfully used to assess the height and, by exploring crown width and tree diameter relationships, the size of individual trees. At the stand level, LiDAR has been used to estimate canopy cover, volume, and biomass and to assess wildlife habitat and fire susceptibility (Means et al. 2000, Naesset 2002, Persson et al. 2002, Andersen et al. 2005, Hinsley et al. 2006, Popescu and Zhao 2007). Continuous technological advancements and intense competition among vendors have resulted in substantial reductions in the cost of acquiring LiDAR data, triggering an explosion of interest in LiDAR technology and prompting discussions on its integration with mainstream inventory operations, such as those conducted by the US Forest Inventory and Analysis program (FIA).

Discrete return LiDAR data consist of a set of points, or "returns," accurately and precisely georeferenced in three dimensions (Baltsavias 1999). These returns are the location where laser pulse energy emitted from a scanning instrument is backscattered off of a target. Returns are identified along the pulse trajectory as local amplitude maxima of backscattered energy in a process known as pulse discretization. Owing to the capacity of small footprint laser pulses to propagate through small canopy openings to the ground and backscatter to the airborne sensor, LiDAR is capable of assessing ground elevation (Kraus and Pfeifer 1998). Assuming adequate return density, the "return cloud" of data points can be processed to detect individual trees (Brandtberg et al. 2003) and to generate digital models of the vegetation canopy surface (canopy surface model [CSM]) and bare ground (digital terrain model [DTM]) (Hodgson et al. 2003, Clark et al. 2004). Estimates of height for individual trees are obtained by subtracting the DTM from the CSM value at selected locations believed to represent the

Demetrios Gatziolis, US Forest Service, Forest Inventory and Analysis Program, PNW, Portland Forestry Sciences Laboratory, 620 SW Main Street, Suite 400, Portland, OR 97205—Phone: (503) 808-2038; Fax: (503) 808-2020; dgatziolis@fs.fed.us. Jeremy S. Fried, US Forest Service, PNW FIA—jsfried@fs.fed.us. Vicente S. Monleon, US Forest Service, PNW FIA—vjmonleon@fs.fed.us.

Acknowledgments: We thank Jeremy Sapp, Brett Annegers, and Mark Terhune for their assistance with the collection of field data used in this study; The Oregon Department of Forestry and the PNW Station Director's Office for funding support; Watershed Sciences, Inc., of Corvallis, Oregon, for information on LiDAR data preprocessing, and the delivery of customized data products; and 12 owners of private forestland in the study area for providing access to their property and logistical support.

Manuscript received September 30, 2008, accepted July 23, 2009

tops of tree crowns. Variants of this approach have yielded height estimates for individual trees that reportedly rival the accuracy of those assessed in the field via conventional mensurational techniques (Hyyppä et al. 2000, Persson et al. 2002, Maltamo et al. 2004, Andersen et al. 2006). However, underestimation of tree height due to inadequate return density, lack of comprehensive pulse coverage of the scanned area, imperfections in the algorithms used to generate the CSM and DTM, and other issues related to pulse penetration into the canopy are also commonly reported (Lefsky et al. 2002, Gaveau and Hill 2003, Yu et al. 2004). Developing suitable corrections for such bias has been challenging because several factors contribute to the underestimation (Hyyppä et al. 2004).

Nearly all evaluations of the suitability of LiDAR for estimating tree heights have been carried out in relatively simple forest conditions with a uniform overstory, little if any understory vegetation, and gentle topography (Naesset 1997, Popescu et al. 2002, Maltamo et al. 2004). These circumstances probably facilitate the extraction of laser-derived descriptions of forest canopy and bare ground that are of high fidelity and, hence, conducive to accurate and precise estimates of tree height. However, such conditions are not common in many forested areas, including the coastal forests of the US Pacific Northwest. For those forests, little is known about the effects that their complex structure and terrain may have on the suitability of LiDAR-derived height estimates. The objective of this study was to conduct a rigorous evaluation of the accuracy and precision afforded by LiDAR-derived estimates of tree height in the structurally complex, high-density and biomass-rich forests growing on the steep slopes of the coastal Pacific Northwest. The evaluation was performed using laser data acquired under both leaf-on and leaf-off conditions and was based on a precise set of calibrated heights obtained in the field via survey-grade instruments.

Sources and Magnitude of Error in LiDAR Tree Height Estimation

Although the estimation of tree height from laser data is conceptually simple, implementation is susceptible to several potential sources of error related to instrument and data acquisition specifications and how the LiDAR data are processed. This study focuses on three sources of error that will always be present: underestimation of tree top elevation, discrepancies induced by tree lean, and overestimation of terrain height (DTM error), along with the interactions among these errors.

Tree top elevation is almost always underestimated because the backscattered laser energy must exceed a discretization threshold before it is sufficient to be identified as a return, and this threshold will not be exceeded until some point deeper in the crown than the highest point of the tree. Error due to tree lean is introduced by the two-dimensional offset between tree base and top of the tree, which is not considered when height is computed as the elevation difference between the return believed to represent the tree top and the point on the DTM surface directly below the tree top. There are no examples known to the authors for which this source of error in LiDAR tree height estimation has been identified, most likely because conditions under which tree lean error becomes especially problematic are uncommon in most biomes. However, these conditions—very tall trees growing on steep slopes—are typical in the temperate rainforests of the Pacific Northwest.

DTM errors are artifacts that emerge from anomalies in the spatial distribution of the return cloud and of the processes that generate terrain models. A key component in DTM generation is to classify laser returns as either on or above the ground, filtering out the aboveground returns before interpolating a ground surface. Return classification errors or failures to identify and remove below-ground returns (Hyyppä et al. 2004) lead to DTM errors. Popular approaches suggested for processing laser return clouds to generate DTMs in forested areas can be classified into three types: iterative approximation (Kraus and Pfeifer 1998, Elmqvist et al. 2001, Kobler et al. 2007), progressive densification (Axelsson 1999, Sohn and Dowman 2002), and morphological filtering (Vosselman 2000, Sithole 2001, Chen et al. 2007).

Under iterative approximation, an initial surface model is generated using last returns or sometimes the entire return cloud. Returns that lie above the surface are assigned weights of magnitude proportional to the inverse of their vertical distance above the surface. Returns under the surface receive weights that increase with their vertical distance below the surface. The weights (low above the surface and high below) are used to influence the surface obtained in the next iteration. Iterations continue until the magnitude of elevation adjustments falls below a user-specified threshold.

In progressive densification, a set of returns identified as local elevation minima within larger areas are classified as ground points and used to obtain a base surface via triangulation. The angles formed between yet unclassified returns, the vertices of the closest triangle, and the triangle's plane are examined. Returns with angles below a user-specified threshold are classified, one at a time, as ground, and the triangulated surface is updated until no more returns with angles below the threshold remain.

There are two variants of morphological filtering. One operates directly on the return cloud and uses a function of distance and elevation to test the realism of elevation differences between neighboring returns assumed to represent the ground. Typically, the form of the function has the rate of elevation change, decreasing with distance and ultimately reaching an asymptote, and functional form, either omnidirectional or aspect-specific and typically derived from terrain training data if available or from assumptions about maximum terrain slope. Aboveground returns that exceed the function limits are eliminated. The second variant works with raster representations of the return cloud, in which the value of each cell is initially set to the elevation of the lowest return present within the cell. The raster is then processed with the morphological operation known as Opening (Haralick et al. 1987), which identifies groups of cells that protrude from (have values consistently higher than) their surroundings. This

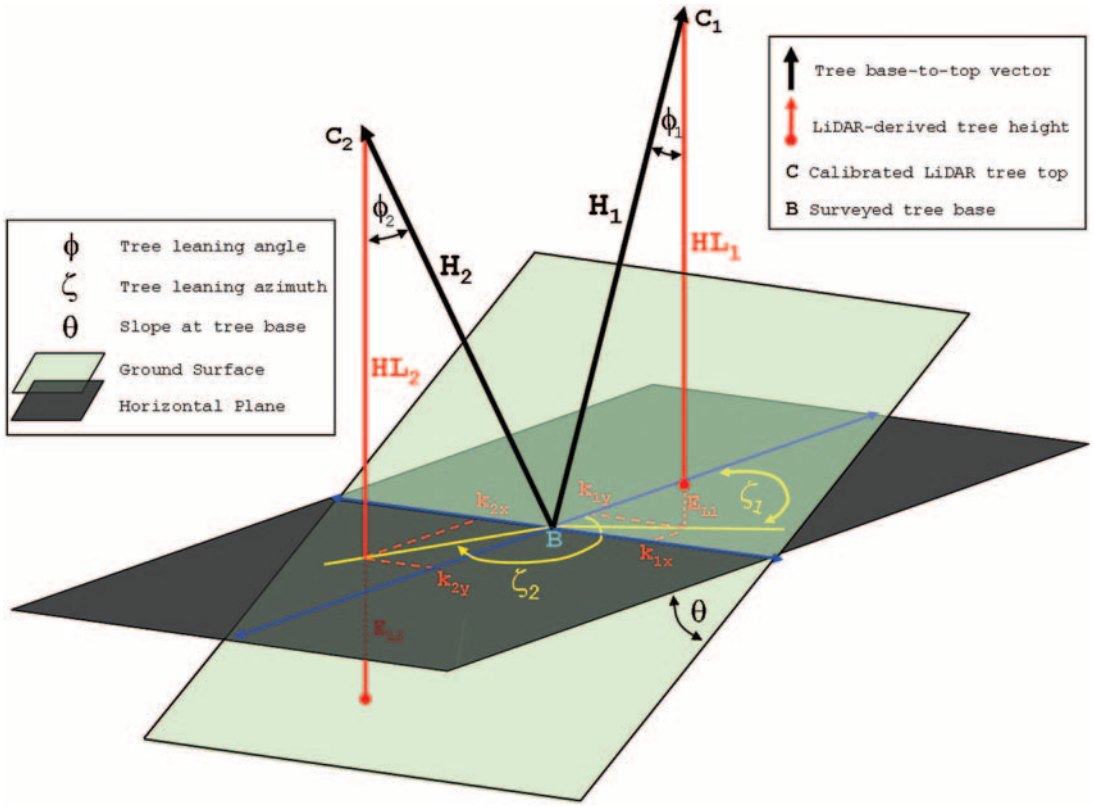

Figure 1. Schematic diagram of the geometry involved in the estimation of tree height. Two trees, the first leaning uphill (H_1) and the second downhill (H_2), are represented with thick black lines. Solid red lines represent the corresponding LiDAR-assessed tree height (HL). Dotted lines represent the vertical distance (E_L) between the projection of a tree top on the ground surface and a horizontal plane. The coordinate system is centered on the tree base so that the *x*-axis coincides with the contour line passing through the base of the tree and the *y*-axis points at the direction of the local aspect. Dashed lines show the offsets of tree tops on a horizontal plane.

is often the case in forested landscapes where the elevation of the lowest return in cells under a tree is well above the ground. Performing the morphological operations using raster windows of progressively larger size and assigning weights to each cell depending on the outcome of the morphological operator for different window sizes allows identification and removal of aboveground objects (Zhang et al. 2003). In the last step, the morphological operations Erosion and Dilation (Haralick et al. 1987) can be used to replace the initial raster values with the filtered elevations (Lohmann et al. 2000). A notable limitation of this approach, the assumption of constant slope, has been resolved by improvements introduced by Chen et al. (2007)

An assumption intrinsic to all types of laser return classification and DTM generation is that the local density of on-ground and aboveground returns is adequate to quantify elevation differences between and ultimately to discriminate between these two groups of returns. On forested land and steep slopes in particular, this assumption may not always hold because the spatial arrangement of ground and vegetation returns there have similar characteristics: large elevation differences within small horizontal distances (Kobler et al. 2007). Consequently, the magnitude of DTM errors and therefore the accuracy of LiDAR-derived terrain models in forested areas have been highly variable. Reutebuch et al. (2003) reported that under coniferous stands and 4 returns m^{-2} density, they observed a root mean square error (RMSE) of 31 cm, whereas Kraus and Pfeifer (1998) reported an RMSE of 57 cm in wooded areas. However, others have reported that it is common to have a positive elevation bias of >1.5 m in more complex vegetation (Hodgson et al. 2003, Clark et al. 2004) and that bias is even greater in sloped terrain (Kobler et al. 2007).

The error budget in laser-based estimation of tree height can be quantified by using a conceptual model that is based in part on the FIA field data collection protocol. According to this model (illustrated graphically in Figure 1), the height of a tree is computed as the magnitude (length) of a vector H originating at the base of the tree and ending at its top. In the FIA data collection protocol the origin and end of vector H are determined visually in the field. Figure 1 shows two instances of H, one for a tree leaning uphill (H_1), and another for a tree leaning downhill (H_2). The LiDAR-assessed tree height is calculated as the magnitude of a perpendicular-to-a-horizontal-plane vector HL connecting the highest crown return and the projection of that return on the DTM generated from the laser data. The error in the assessment of tree height (or height bias) E_H is computed as

$$E_H = |HL| - |H|, \quad (1)$$

where $|HL|$ and $|H|$ are the magnitudes of vector HL and H representing the LiDAR-derived and field-assessed tree

heights, respectively. Assuming no positional discrepancy between the true and LiDAR-identified tree tops, the angle ϕ formed between vectors H and HL (Figure 1) quantifies the amount of tree lean:

$$\phi = \arccos\left(\frac{h * hl}{|H| * |HL|}\right), \quad (2)$$

where h and hl are the unit-normalized version of vectors H and HL, respectively. The ends of vectors H and HL usually do not coincide, and, therefore, the angle ϕ computed by using Equation 2 is an approximation. For leaning trees, E_L is the component of laser-derived tree height HL corresponding to the vertical distance between the projection of a tree top to the laser DTM and to the surveyed ground:

$$E_L = H * \sin\phi * \cos\zeta * \tan\theta, \quad (3)$$

where ζ is the horizontal angle formed by vector HL relative to the direction of the local aspect, and $\tan\theta$ is the local ground slope, which is assumed to be constant in the vicinity of the tree base. The intersection of the slope and horizontal planes approximates a contour line passing through the tree base. The total error in LiDAR-assessed tree height is therefore a function of the accuracy and precision of the laser-derived DTM and the bias in determining the elevation of the true tree top and, for leaning trees, has a component affected by the lean angle, the local slope, and the height of the tree (Figure 1). Hence, the error E_H in the laser-assessed height of individual trees can be calculated as

$$E_H = E_{\mathrm{DTM}} + E_T + (E_L|\phi > 0) + \varepsilon, \quad (4)$$

where E_{DTM} is the error in the estimation of ground elevation, E_T is the bias in the elevation of identified tree tops, E_L is the error due to lean by angle ϕ, and ε is the amount of error contributed by discrepancies between the true and LiDAR-assessed tree top.

Methods

Study Area

The 9,500-ha study area, located in the Oregon Coast Range, USA (Figure 2), is centered at approximately 44°32′N, 123°39′W. More than 90% of the area is temperate rainforest, with mean annual precipitation of 2000 mm. Forty-seven percent of the forests are privately owned and intensively managed for timber production. Approximately 1,550 ha are managed by the Oregon Department of Forestry and 3,850 ha by the Siuslaw National Forest, although recent activity on the National Forest has been limited to relatively infrequent precommercial thinning, mostly before 1984. Forests are composed primarily of Douglas-fir (*Pseudotsuga menziesii* [Mirb.] Franco), bigleaf maple (*Acer macrophyllum* Purch), and red alder (*Alnus rubra* Bong.), with the hardwoods usually dominating areas adjacent to the drainage network. Elevation ranges from 66 to 1,123 m above sea level and terrain is characterized by steep slopes. Within the forested portions of the study area, mean slope is 61% and the 75th percentile slope is 84%.

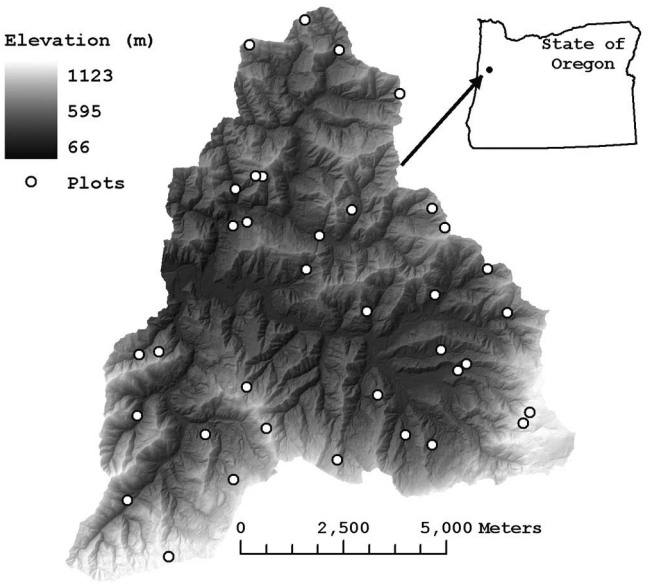

Figure 2. Elevation map of the study area, presented as shaded raster, showing the locations of field plots. Because of confidentiality considerations, nine plots have been omitted.

Field Data

Forty-five fixed-area, 15-m radius plots were established in summer 2005, distributed across forest type classes (conifer, hardwood, and mixed), tree size, and stand density. All trees with dbh exceeding 12.7 cm or of dominant or codominant status regardless of dbh were tallied in each plot. For each tree, the species and dbh were recorded, and the projection of its crown was delineated by measuring distance and azimuth from the tree base to the edge of the crown and then fitting a spline between the measured locations (Figure 3). Continuous feedback from field crew members guided a person operating a clinometer to on-ground locations that defined the shape of each crown. The use of a clinometer ensured that the operator was positioned directly below the edge of the crown being delineated. Two dominant trees in each plot were bored to determine age, except in the recently planted Douglas fir and young alder plots. Sketch maps depicting the presence, type, and height of understory vegetation were produced. Tree height was measured using an electronic clinometer/distance finder from multiple viewing locations. The minimally acceptable precision of tree heights obtained in the field was a priori set to not exceed an RMSE of 1%. However, estimates of tree height were assigned a precision-class code reflecting the crew's confidence in the estimate (e.g., as affected by visibility of the tree top from the ground). The high frequency of low precision codes in close-canopy stands confirmed concerns that, in such conditions, traditional field mensuration techniques would fall short of the precision required for this study. This finding motivated an alternative approach to obtaining "true" height that entailed a highly precise terrain survey and calibration of the tree crown tops in each plot. The tree top calibration was performed at 23 additional sites, located along the edge of stands exposed by recent clearcuts, next to sizable canopy openings, or next to land dominated by young or recently

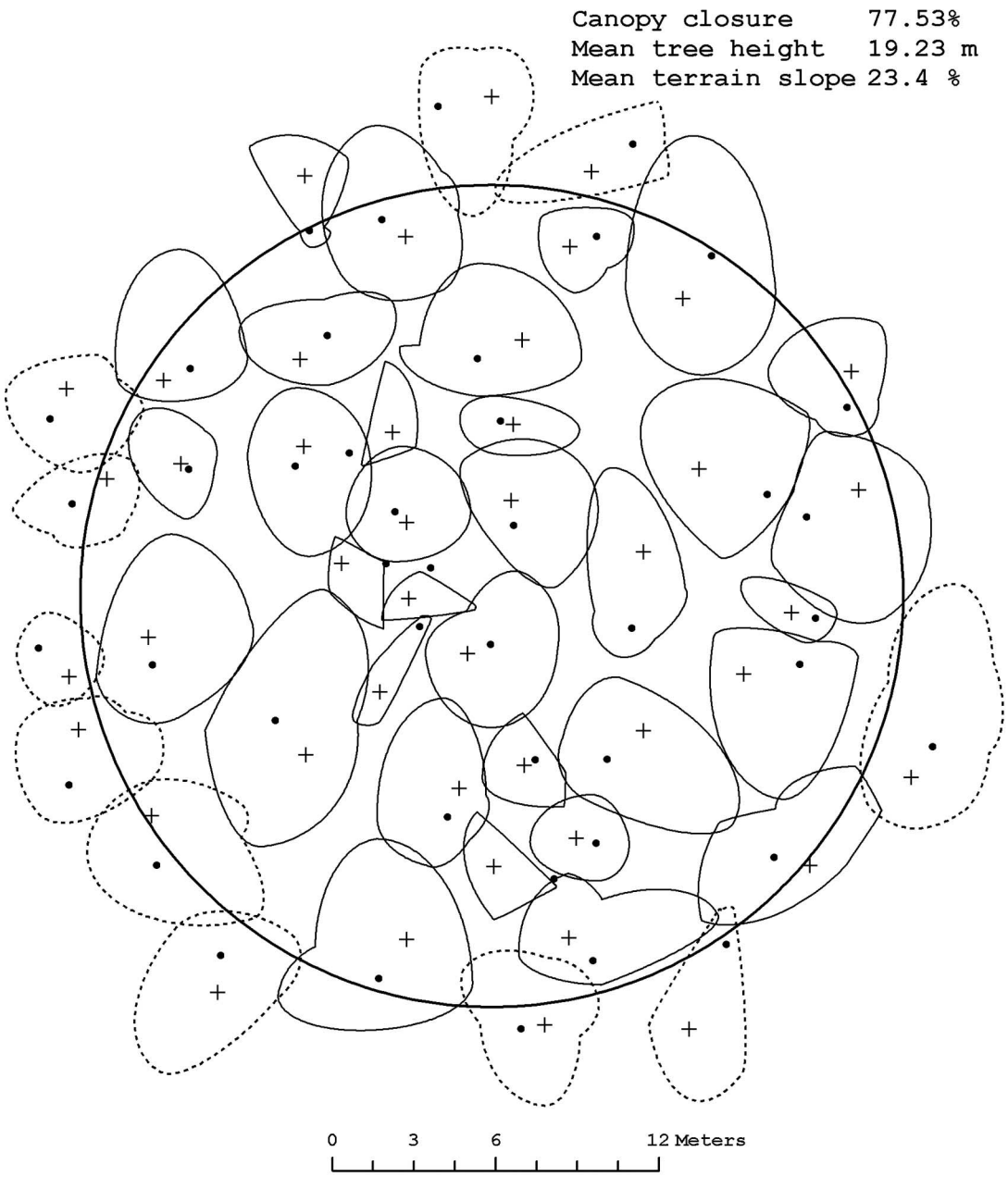

Figure 3. Field-delineated crowns, surveyed tree bases (●), and LiDAR-assessed tree tops (+) of a plot in a deciduous stand with medium canopy cover. The thick line represents the boundary of the 15-m-radius plot. Crowns of trees with base outside of the plot are represented with dashed lines.

planted trees. The tops of the tall trees were surveyed during windless days, with the total station, from three reference positions previously surveyed with a Real-Time Kinematic (RTK) global positioning instrument. The methodology used is based on triangulation and is similar to that detailed by Andersen et al. (2006). By computing the three-dimensional location of a tree top from three vintage points, the measurement error could be assessed. Trees with measurement RMSE of the location of their tops exceeding 7.5 cm were eliminated from further consideration. The height of short trees (<3 m) was measured with a calibrated pole. A comparison of the coordinates of the surveyed tops to the coordinates of colocated (within 2 m in two dimensions) highest LiDAR returns for 220 trees (120 conifers and 100 hardwoods) of various sizes and ages revealed bias in the elevation of tree tops obtained by processing the LiDAR data. The mean tree top bias E_T for hardwoods, conifers, and each laser data acquisition timing (leaf on and leaf off) was subsequently computed.

Plot Registration and Ground Survey

For each plot, at least two locations were precisely referenced by using the RTK instrument at leaf-off conditions. The instrument was set to record only when the expected, internally calculated, three-dimensional precision was better than 5 cm. Because the operation of the RTK instrument is limited to areas free from overstory vegetation, in 36 plots the closest two locations successfully recorded with the

RTK were in canopy openings well outside the plot boundary. For those plots, transects connecting reference locations to corresponding plot centers were established and surveyed with a total station. For the remaining 9 plots, unobstructed, undercanopy lines of sight between the RTK reference locations and the plot centers supported direct plot georeferencing via the total station. Additional RTK reference locations and transects installed in 12 of the plots revealed that the location error of the plot center ranged from 3.4 to 12.3 cm (mean 5.4 cm), a precision that was deemed acceptable. With the total station positioned and oriented on the plot center, terrain inflection points were flagged over the plot area and a 5-m buffer around the plot. The flag density was higher in portions of the plots exhibiting variations in microtopography. Across plots, the average density was 0.38 points m^{-2}. The flagged locations in each plot were processed to generate 1-m DTMs via kriging (Goovaerts 1997) using 6 nearest neighbors. Alternative DTMs generated via inverse distance weighting with a power factor of 2 and via Delaunay triangulation-derived irregular networks later converted to their raster equivalent via cubic convolution compared closely with the kriging-derived DTM. The mean absolute difference between the kriging-derived DTM and alternative methods was <2.5 cm and visualizations of the difference surfaces showed no spatial patterns. Hence, the alternative DTMs were not considered further. The precision of the kriging-derived DTMs was evaluated using cross-validation that excluded one ground return per plot each time and compared its surveyed elevation to the interpolated value. The mean DTM interpolation error across plots was 3.9 cm.

LiDAR Data

Laser scanning data were acquired at leaf-on conditions in July 2005 and leaf-off conditions in February 2006 using, in both acquisitions, an aircraft-mounted Optech 3100 system from a nominal height of 1,000 m aboveground level. The LiDAR instrument operated on a 71-kHz laser repetition rate and captured a 20° scan width (10° from nadir) with adjacent flight line overlap of 50%. Laser data had a mean density of 7.52 returns/m^2 for the leaf-on mission and 8.70 returns/m^2 for the leaf-off mission. For both missions the spot spacing was 32 cm with nominal laser footprint diameter of 33 cm. Pulse discretization to individual returns enforced a minimum distance of 3 m between a first and a second return and 2 m between subsequent returns. A maximum of four returns could be identified from a single pulse. Compared with horizontal, impermeable surfaces surveyed with the RTK, the laser returns had an RMSE of 2.6 cm during the leaf-on mission and 3.1 cm during the leaf-off mission. For each mission, the vendor delivered both raw (unfiltered) data and a filtered version that contained only returns classified as either on-ground or aboveground. Filtering was performed using an adaptive triangulation irregulated networks model (Axelsson 1999) implemented in the TerraScan software. An initial ground surface was obtained via triangulation performed using only returns that featured the lowest elevation within rectangular, 0.1-ha regions. Surface densification was limited to a minimum horizontal distance of 1.4 m between returns and angular offset of 5°. Ground surfaces produced with these default filtering values were evaluated visually against the unfiltered return cloud for each of the 1-km^2 data tiles. Where apparent filtering errors were identified, the vendor repeated the process with modified settings until the ground surface produced was free of obvious errors. We generated 1-m plot DTMs using the filtered returns classified as representing the ground via kriging with 6 nearest neighbors.

Alternative plot DTMs were generated using the unfiltered return cloud and the TreeVis (Weinacker et al. 2004) and TIFFs (Chen 2007) software packages. Return filtering in TreeVis is enabled by an iterative approximation algorithm that we executed with default settings. TIFFs applies morphological filtering and includes a preprocessing step designed to remove artifacts (below-ground returns). Plot DTMs for combinations of algorithmic parameter thresholds in TIFFs were obtained. All LiDAR- and field survey-derived DTMs had the same resolution (1 m) and were co-registered. Simultaneous three-dimensional renditions of the raster surfaces and unfiltered returns performed in FUSION software (McGaughey 2009) enabled visual pair-wise comparisons of field-surveyed and TreeVis- and TIFFs-derived DTMs. In addition, FUSION-enabled visualizations of the return clouds for selected plots were presented to four human operators who, working independently, were asked to delineate the ground surface along two, 1-m wide, transects for each plot. Transects were oriented in parallel and across elevation contour lines. The task was facilitated by custom return cloud rotation that enhanced the perception of depth. In the absence of any other information or reference, manual filtering is regarded as the best possible classification into ground and off-ground returns (Kobler et al. 2007) and is often used to compare filtering algorithms (Sithole and Vosselman 2004).

For nearly half the plots at leaf-on conditions and approximately two-thirds of the plots at leaf-off conditions, the visual comparison revealed no noticeable elevation differences between the survey- and the laser-derived DTMs as discrepancies were small and dispersed within the plots. For the remaining plots, discrepancies were typically larger for the DTMs generated with TreeVis, which exhibited a tendency to generalize local terrain features. TIFFs-derived DTMs were sensitive to even small changes in input parameter values, occasionally produced surfaces with a stair-step appearance, and sometimes had substantial variability in accuracy within a single plot. DTMs generated using the TerraScan-filtered returns were consistently equal to or more accurate than the alternatives, although for several plots they contained substantial positive elevation bias. For the rest of the analysis, we considered only the TerraScan-derived DTMs. Their accuracy was estimated by comparing cell values to the elevation of 50, randomly chosen, surveyed locations within each plot.

Estimation of Tree Height, Terrain Derivatives, and Canopy Cover

To determine the heights of dominant and codominant trees in each plot, the field-delineated crowns were first

overlaid with the return cloud. The elevation of the highest return within a crown, identified using leaf-on laser data, was recorded and subsequently adjusted to account for the bias E_T observed at the exposed stands. E_T was computed as the mean leaf-on elevation discrepancy between surveyed and LiDAR-derived tree top locations, independently for conifers and hardwoods. The heights obtained after this adjustment are referenced here as "calibrated." The angle θ used in the computation of local ground slope was defined as the one formed between a plane $p(x, y, z)$ fitted via least squares to the flagged locations present horizontally within 5 m from the base of the tree and a horizontal plane $p(1, 1, 0)$. It was computed as

$$\theta = \arccos\left(\frac{\sqrt{2}}{2}\frac{(x+y)}{\sqrt{x^2+y^2+z^2}}\right). \quad (5)$$

Tree heights and terrain derivatives (local slope and aspect at the base) were computed for a total of 1,009 trees. The total height error and its components were calculated according to the error-source model presented earlier. The magnitude of error component ε was assessed via simulation that entailed horizontal jittering of the LiDAR-identified tops in random direction 100 times per tree, calculation of E_H (Equation 1) for each jittering instance, and computation of the root mean square discrepancy to the E_H of the nonjittered tree top. The jittering distances were drawn from distributions whose moments were forest type- and laser acquisition timing-specific and matched those of the corresponding distributions of horizontal discrepancies between observed and LiDAR derived-tree tops in the 23 plots used for tree top calibration. The maximum jittering distance was 0.43 m for conifers, 0.98 m for hardwoods and leaf-on data, and 1.43 m for hardwoods and leaf-off laser data. The random relative azimuth between the LiDAR-derived and true tree tops observed in the 23 calibration plots suggests that any height bias induced by error in the location of LiDAR-derived tops will probably be balanced at the plot level. Because of this observation and the fact that the magnitude of ε assessed with the simulation was $<1\%$ of H for $>94\%$ of the trees (the rest were short saplings growing on 80+% slopes), the contribution of ε in determining E_H (Equation 4) was deemed negligible and was not further considered. We applied regression analysis to evaluate each of the error components in Equation 4 independently and in reference to plot vegetation parameters such as forest type, tree size, density, canopy cover, and local topography.

An estimate of canopy cover for each plot was obtained by considering the field-delineated crown projections of dominant and codominant trees (crowns were regarded as opaque) and calculating the portion of the plot area covered by them. To evaluate the consistency of crown delineation and therefore the accuracy of canopy cover estimates obtained, crown delineation was repeated several weeks after the initial field visit for seven plots. The estimates of canopy cover obtained at the second field visit did not differ from those obtained at the first visit by $>2.8\%$ (mean difference was 2.1%). Plot overlays of the crowns delineated in each visit produced only sliver (thin and usually long) polygons representing lack of correspondence in the assessments with maximum width of only 10–20 cm. Such minimal disagreement between independent assessments of crown perimeter confirms the high precision of the crown delineation effort. Note that our definition of canopy cover refers to the planimetric projection of the canopy onto the ground and thus differs from what would be obtained, for example, via hemispherical photography (e.g., percent sky as viewed from a given location on the ground) under the canopy in that crowns are not opaque and overlapped crowns would tend to produce higher canopy cover estimates.

Results

We present results by source of tree height assessment error (E_T, E_L, and E_{DTM}) and for the total height error E_H summarized at the plot level and in relation to forest type.

Tree Top Error

The tree top calibration data collected in the 23 sites revealed a bias of -0.59 m for conifers in both acquisitions. For hardwoods the absolute magnitude of the bias increased from -0.29 m at leaf-on to -0.58 m at leaf-off conditions (Figure 4). A paired t test of the elevation differences between the observed and LiDAR-derived tree tops was significant at $\alpha = 0.05$. There was no evidence in the calibration data that the magnitude of the height bias was related to the height of the tree or the size of its crown. The mean two-dimensional (horizontal) discrepancy between surveyed and LiDAR-identified tree tops for conifers was 11 cm at leaf-on and 10 cm at leaf-off conditions. For hardwoods the discrepancy was larger: 25 cm using leaf-on laser data and 36 cm with leaf-off data.

Tree Lean Error

Most of the trees inventoried in this study were leaning. Of the 775 trees that were taller than 3 m, for only 12% was the horizontal location of the LiDAR-identified top within 33 cm (the mean width of a LiDAR pulse footprint) of the base. The mean tree base-to-top horizontal offset was oriented downhill and was longer for coniferous species (1.19 m) than for hardwoods (0.95 m). Lean direction on one sixth of the trees (16.2% of conifers and 16.6% of hardwoods) was within 45° of the steepest uphill gradient, whereas on 38% of conifers and 42.5% of hardwoods it was within 45° of the steepest downhill gradient (Figure 5). Variability in lean direction relative to the local aspect and the magnitude of lean angle ϕ was greater among than within plots for conifers and relatively stochastic for hardwoods.

In 22 of the 42 plots (52%) with mean calibrated tree height ($\bar{H}$) > 3 m, the mean per plot height error due to tree lean ($\bar{E}_L$) exceeded 1 m. In 24 plots (57%) $\bar{E}_L$ exceeded 5% of $\bar{H}$. The within-plot variability in individual tree error was substantial for all forest types and tree sizes. In 27 plots (64%), the range of individual tree E_L was larger than 5% of $\bar{H}$ (Table 1). Although the error E_L contributed in the LiDAR-assessed tree height by tree lean is a function of the calibrated tree height H (Equation 3), scattergrams of E_L and H showed no significant association between error and

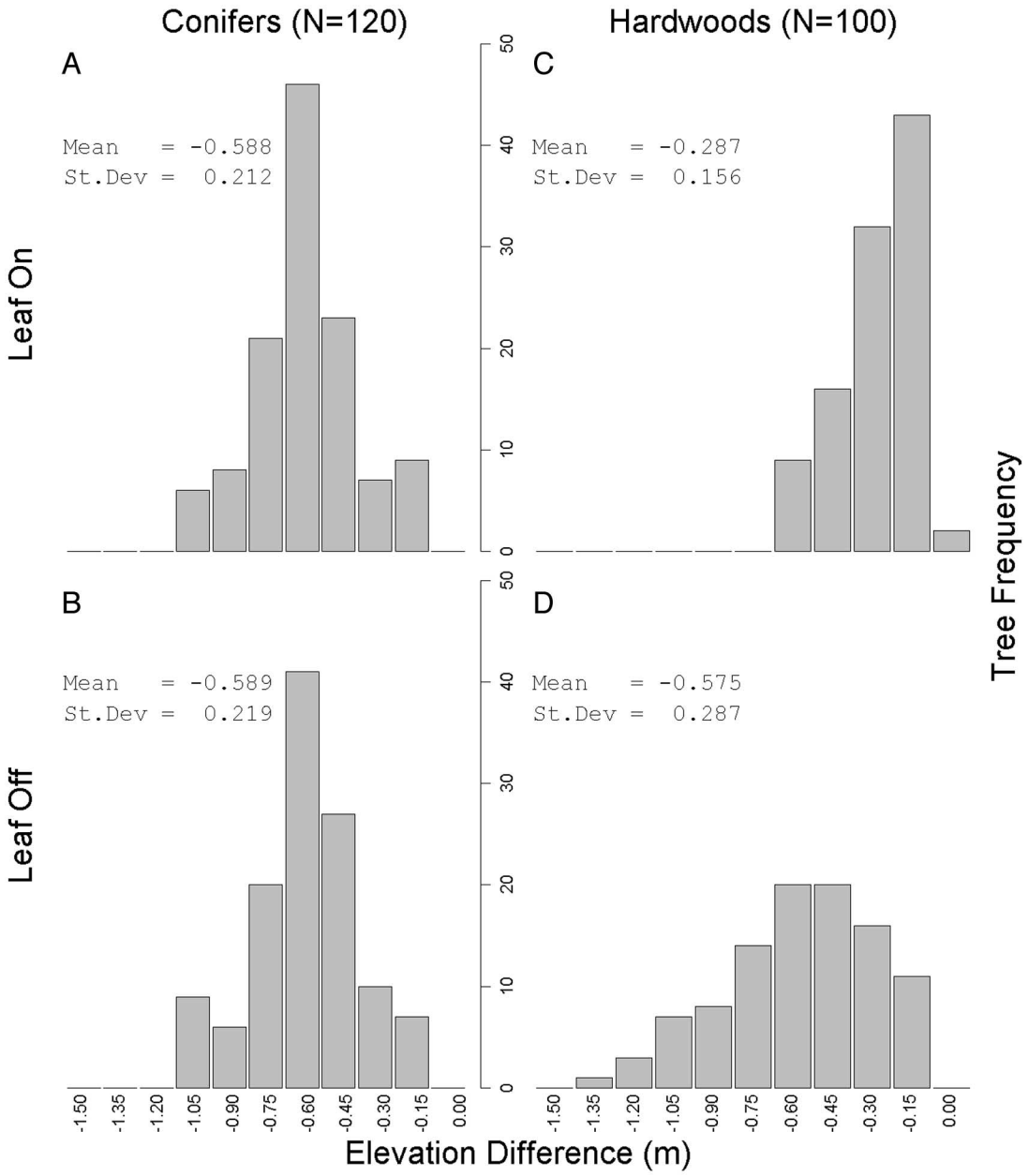

Figure 4. Histograms of elevation discrepancies between surveyed and LiDAR-derived tree top locations.

height for all combinations of leaf-on and leaf-off data and plot forest type. Slope, stem density, canopy cover, and tree crown diameter were not related to E_L.

DTM Error

Comparisons between LiDAR-derived and surveyed plot DTMs revealed substantial variability in the accuracy and precision of terrain descriptions extracted from the laser data. The precise ground representation evident in low canopy cover (<60%) plots degraded quickly at higher levels of canopy cover. The laser DTM accuracy was affected by the timing of the laser data acquisition (leaf-on and leaf-off), forest type, canopy cover, and, for conifers only, stem density. As a result, in 23 of 45 plots (51%), overestimation of DTM elevation calculated by using leaf-on laser data led to an underestimation of mean tree height $\bar{H}$ by >5% (Table 2), whereas in 8 plots (3 coniferous, 1 mixed, and 4 hardwoods), the underestimation exceeded 20% of H. In 21 of these 23 plots, E_{DTM} was larger than 1 m. Owing to better penetration of hardwood tree crowns at leaf-off conditions, the percentage of plots with $\bar{E}_{\mathrm{DTM}} > 0.05\ \bar{H}$ was reduced to 35.5. In 2 hardwood plots the underestimation of $\bar{H}$ by >5% of mean height persisted even when leaf-off laser data were used (Table 2).

$\bar{E}_{\mathrm{DTM}}$ was found to correlate positively to canopy cover (higher canopy cover, as measured on the ground during leaf-on conditions, generally led to greater overestimation of elevation) for all forest types, except for hardwood plots at leaf-off where, not surprisingly, the association was weak (Figure 6). Where canopy cover was below approximately 80%, the DTM accuracy for coniferous plots was <0.5 m. At higher levels of canopy cover, overestimation of ground elevation and therefore underestimation of tree height increased markedly. The R^2 (coefficient of determination)

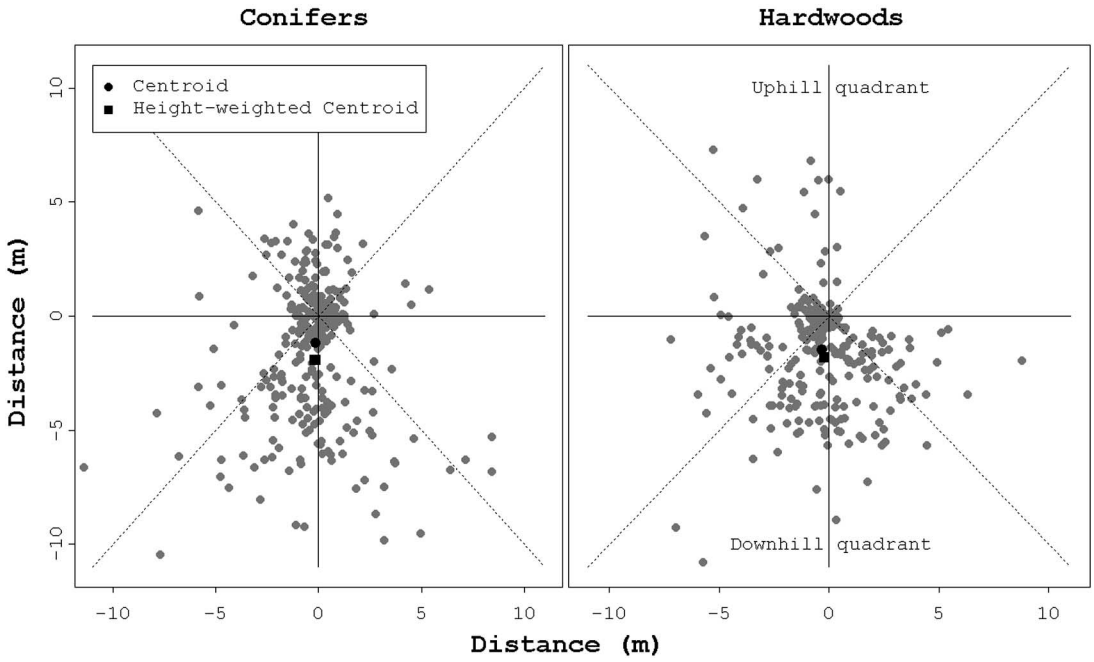

Figure 5. Horizontal position of LiDAR-calibrated tree tops relative to surveyed bases of corresponding trees for coniferous and hardwood species. Tree bases are centered at the coordinate origin, the *x*-axis is parallel to the contour line passing from each tree base, and the positive *y*-axis is oriented uphill. Dashed lines split the horizontal plane into quadrants.

Table 1. Plot membership in classes of mean tree-height assessment error ($\bar{E}_L$) magnitude and plot forest type

		No. plots		
Plot forest type	Plot $\bar{E}_L$	Total	Plot $\bar{E}_L$ >5% plot $\bar{H}$	Plot E_L range >5% plot $\bar{H}$
Coniferous	<−1 m[a]	2	2	2
	−1 to 1 m[b]	9	1	4
	>1 m[c]	6	5	4
Total		17[d]	8	10
Mixed	<−1 m[a]	2	2	2
	−1 to 1 m[b]	5		1
	>1 m[c]	4	4	4
Total		11	6	7
Hardwoods	<−1 m[a]	1	1	1
	−1 to 1 m[b]	6	2	2
	>1 m[c]	7	7	7
Total		14	10	10
Total	l	42	24	27

E_L is induced by tree lean and is embedded in LiDAR-derived estimates of mean plot tree height ($\bar{H}$).
[a] Height underestimation (uphill tree leaning).
[b] Little or no tree height underestimation.
[c] Height overestimation (downhill tree leaning).
[d] Plots with mean height below 3 m are not included.

obtained by second-order polynomial regression of $\bar{E}_{\mathrm{DTM}}$ on plot canopy cover was 0.58 at leaf-on and 0.54 at leaf-off conditions, and both regressions were significant at $\alpha = 0.01$. Owing to two plots with low tree canopy cover but very dense, 1- to 2-m-tall understory vegetation, there was no significant correlation between mixed vegetation plots and laser DTM error at leaf-on conditions ($R^2 = 0.11$, $P > 0.1$). With these two plots removed, the linear regression significance and fit was improved ($R^2 = 0.65$, $P < 0.01$). The positive correlation between DTM error and canopy cover for mixed plots persisted at leaf-off conditions ($R^2 = 0.50$, $P < 0.01$) (Figure 6). Ten of the 14 hardwood plots exhibited a strong linear relationship between DTM error and canopy cover ($R^2 = 0.95$, $P < 0.01$). Including the remaining four hardwood plots in the regression led to a substantial reduction in fit ($R^2 = 0.43$), but the regression remained significant at $\alpha = 0.01$. These four plots, all with canopy cover >75% and DTM overestimation <1.5 m, differed from the remaining hardwood plots with comparable canopy cover in that they contained small canopy openings, either within or very close to their boundaries, with sparse understory vegetation (Figure 6).

Of the remaining vegetation and topography parameters examined, only $\bar{H}$ of coniferous plots was found to correlate to DTM error, but the relationship was complex. Plots with

Table 2. Plot membership in classes of laser-derived mean DTM error ($\bar{E}_H$) magnitude and forest type

		No. Plots			
		Leaf-on acquisition		Leaf-off acquisition	
Plot forest type	Plot $\bar{E}_H$	Total	Plot $\bar{E}_H > 5\%$ plot $\bar{H}$	Total	Plot $\bar{E}_H > 5\%$ plot $\bar{H}$
Coniferous	<-1 m[a]	9	9	9	9
	-1 to 1 m[b]	11		8	
Total		20	9	17	9
Mixed	<-1 m[a]	5	5	3	2
	-1 to 1 m[b]	6	1	8	2
Total		11	6	11	4
Hardwoods	<-1 m[a]	7	7	1	2
	-1 to 1 m[b]	7	1	13	1
Total		14	8	14	3
Total		45	23	45	16

For each plot DTM error was evaluated under LiDAR-identified tree tops and is expressed in absolute terms and relatively to mean plot height ($\bar{H}$).
[a] DTM elevation overestimation leading to height underestimation.
[b] Limited or no bias.

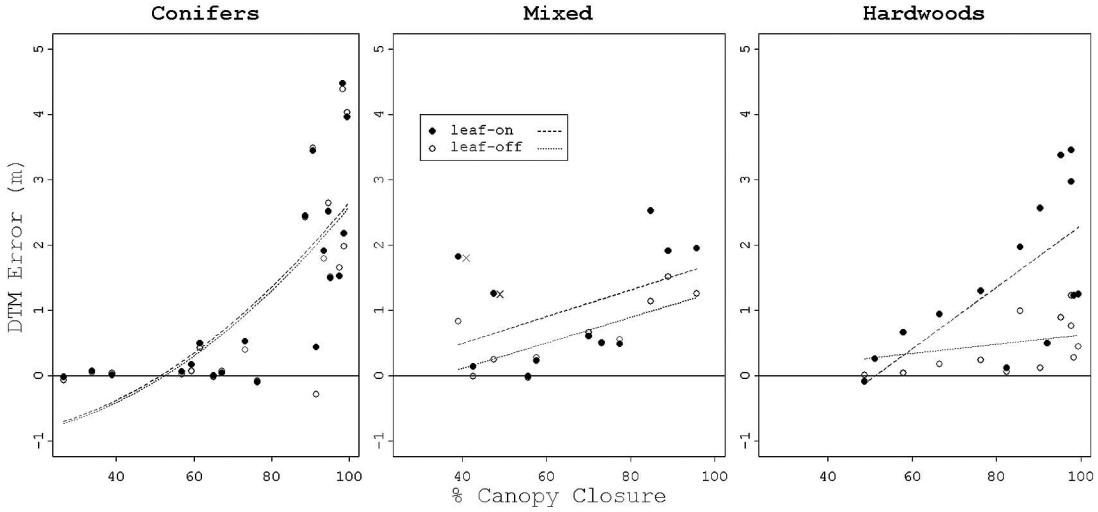

Figure 6. Scattergrams of mean per plot error present in LiDAR-derived digital terrain models using leaf-on and leaf-off data in classes of plot cover type and polynomial regression curves of the error fitted on plot canopy cover. X marks indicate plots with rigorous, very dense understory vegetation. For many plots, the leaf-on and leaf-off error values similarity causes symbol overlap.

mean height of dominant and codominant trees greater than approximately 30 m, had small, positive DTM error, always <1 m, whereas plots with short (<3 m), recently planted Douglas fir trees were practically free of DTM errors. Plots with mean tree height between those heights exhibited substantial DTM overestimation with error ranging between 1.5 and 4.5 m.

Total Error

The magnitude of E_H varied substantially among plots and often even among the dominant and codominant trees on the same plot (Figure 7). The contribution to E_H from bias in the assessment of ground elevation (E_{DTM}) was greater than that of tree lean (E_L) in 13 coniferous, 5 mixed, and 7 hardwood plots when leaf-on laser data were used. At leaf-off conditions, the magnitude of E_{DTM} exceeded that of E_L in 13 coniferous, 3 mixed, and 4 hardwood plots.

In coniferous plots, height error E_H for plots with medium or low canopy cover and short trees (numbered 1, 2, 3, and 10 in Figure 7A) was nearly equal to the bias in tree top elevation owing to very small values of E_{DTM} and E_L. On 3 other plots (4, 7, and 9), accurate DTMs and predominantly downhill tree lean resulted in overestimation of mean plot height by 2–4 m. Elsewhere, accurate DTM extraction and heterogeneous lean direction (plots 5, 8, and 13) kept E_L <1 m, although height error for individual trees was larger, between 3 and 4 m. Height on plots with minimal tree lean, dense canopy, and high-biased elevation estimates (plots 11, 12, 15, and 16) was underestimated by an amount approaching the DTM bias. The DTM bias on three high-canopy-cover plots (14, 17, and 18) was either neutralized or mitigated by predominantly downhill lean. In two high-canopy-cover coniferous plots (19 and 20), substantial DTM overestimation and predominantly uphill lean directions resulted in extreme underestimation of tree height. The large range of E_L values for trees in plot 19, >6 m for leaf-on and >5 m for leaf-off conditions, is attributed to two factors: lean angle was highly variable (a few trees were leaning uphill

Table 3. Frequency of trees and plots with laser-derived height estimation error exceeding 10% of the calibrated individual tree and plot mean height for combinations of laser data acquisition timing and plot forest type

Acquisition timing	Forest type	No. trees with abs(E_H/H) >0.1 (% total)	No. plots with abs($\bar{E}_H/\bar{H}$) >0.1 (% total)
Leaf-on	All	547 (59.5)	18 (42.9)
	Conifers	236 (59.3)	7 (41.2)
	Mixed	112 (51.6)	4 (36.4)
	Hardwoods	199 (65.5)	7 (50.0)
Leaf-off	All	507 (55.2)	16 (38.1)
	Conifers	239 (60.0)	7 (41.2)
	Mixed	98 (45.2)	3 (27.3)
	Hardwoods	170 (55.9)	6 (42.9)

E_H and $\bar{E}_H$, height estimation error; H, individual tree height; $\bar{H}$, mean height.

much more than others), and plot center coincided with the inflection point of the slope's profile curvature. The abrupt change in true local slope, absent in the laser DTMs for both acquisitions, led to more pronounced error in laser-derived tree height estimates for trees with bases near the center of the plot.

In mixed-vegetation plots, absence of tree lean and accurate DTMs (plot 26) or compensation of DTM overestimation by moderate (plots 23, 27, and 28) or more pronounced (plots 21 and 29) downhill tree lean held E_H to $<$1.5 m (Figure 7B). Accurate DTM estimation, low canopy cover, and trees leaning downhill led to positive tree height bias between 1.5 and 3 m for two plots (22 and 25), whereas downhill tree leaning coupled with DTM overestimation caused substantial negative height bias in two other plots (24 and 31). The laser-derived DTMs for plot 30, which is characterized by extended tree crown overlap of taller Douglas fir trees and shorter but codominant hardwoods, high canopy cover, and small lean angles, retained at leaf-off conditions most (1.5 m) of the positive elevation error (2.0 m) calculated at leaf-on conditions. This observation is perhaps an indication that where the spatial arrangement of overlapping coniferous and hardwood crowns exhibits regularity and the grouping of hardwood crowns into clumps is rare, pulse penetration through the canopy to the ground may be limited even at leaf-off conditions.

Within-plot variation in tree height estimation error in hardwoods was much greater than that for the other two forest types, with a range that exceeded 4 m for one in every three hardwood plots (Figure 7C). Where low or medium canopy cover permitted the extraction of DTMs accurate to $\leq$1 m (plots 32–37), the difference in $\bar{E}_H$ between acquisitions was comparable in magnitude to the difference in the tree top elevation calibration between leaf-on and leaf-off conditions. Owing to substantial downhill tree lean, two of these plots (33 and 37) exhibited large height overestimation, whereas a third (plot 34) with trees leaning uphill exhibited height underestimation. In closed-canopy plots, the substantial underestimation of tree height caused by DTM overestimation was partially (plots 38 and 42–45), fully (plots 39 and 40), or even overcompensated for by strong downhill lean. Variability in the magnitude of ϕ and leaning azimuth angle ζ for trees in plots 41–43 produced a large (5+ m) range in individual tree E_H.

Excluding all trees shorter than 3 m, individual tree E_H exceeded 10% of H for nearly 60% of the trees; for hardwood trees the percentage was even higher (Table 3). Compared with individual trees, the percentage of plots with $\bar{E}_H$ $>0.1\ \bar{H}$ was lower (42.9%), mainly because of trees leaning in opposite directions, thereby reducing their $\bar{E}_L$ contribution to the mean plot height error $\bar{E}_L$. Improvement in the DTM accuracy obtained by switching from leaf-on to leaf-off laser data reduced the percentage of hardwood trees that exceeded the 10% height error threshold by nearly 10 points and the percentage of trees in mixed plots by >6 points. The error in one mixed and one hardwood plot was reduced to $<$10% of the mean plot height. Despite these improvements in height estimation accuracy, mean height error at the plot level remained substantial and exceeded the 10% threshold for more than one in every three plots (Table 3).

Regressed linearly against leaf-on E_H, plot canopy cover was found to correlate negatively to and explained a little more than one-quarter of the total variability in the LiDAR-derived estimates of mean height for coniferous plots, hardwood plots, and for all plots combined. The correlation between mean plot height error $\bar{E}_H$ and canopy cover was

Table 4. Parameters and goodness-of-fit measures for linear regressions of laser-derived mean plot tree-height estimation error on plot canopy cover and mean height for combinations of laser data acquisition timing and plot forest type

Acquisition timing	Forest type	Regression structure	R^2	Regression P value
Leaf-on	All	$\bar{E}_H = 2.93^{b} - 0.0527\ CC^{c}$	0.27	$<$0.001
	Coniferous	$\bar{E}_H = 1.49\text{–}4.022 \times 10^{-4}\ CC^{2a}$	0.30	0.008
	Mixed	$\bar{E}_H = 1.77\text{–}5.6 \times 10^{-4}\ CC^{2a}$	0.41	0.021
	Hardwoods	$\bar{E}_H = 3.84\text{–}0.0588\ CC^{a}$	0.28	0.032
	All	$\bar{E}_H = -1.91^{c} + 0.0485 \times \bar{H}^{a}$	0.08	0.033
	Conifers	$\bar{E}_H = -1.99^{b} + 1.148 \times 10^{-4}\ \bar{H}^{2b}$	0.30	0.007
Leaf-off	All	$\bar{E}_H = 1.24^{a}\text{–}3.146 \times 10^{-4}\ CC^{2b}$	0.20	0.001
	Conifers	$\bar{E}_H = 1.52\text{–}3.972 \times 10^{-4}\ CC^{2b}$	0.28	0.010
	Mixed	$\bar{E}_H = 4.06\text{–}0.0708 \times CC^{a}$	0.39	0.024
	All	$\bar{E}_H = -1.67^{b} + 0.0506\ \bar{H}^{a}$	0.10	0.021
	Conifers	$\bar{E}_H = -1.96^{b} + 1.178 \times 10^{-3}\ \bar{H}^{2b}$	0.31	0.007

$\bar{E}_H$, mean plot tree-height estimation error; CC, canopy cover; $\bar{H}$, mean height.
[a] Significance level: 0.050.
[b] 0.010.
[c] 0.001.

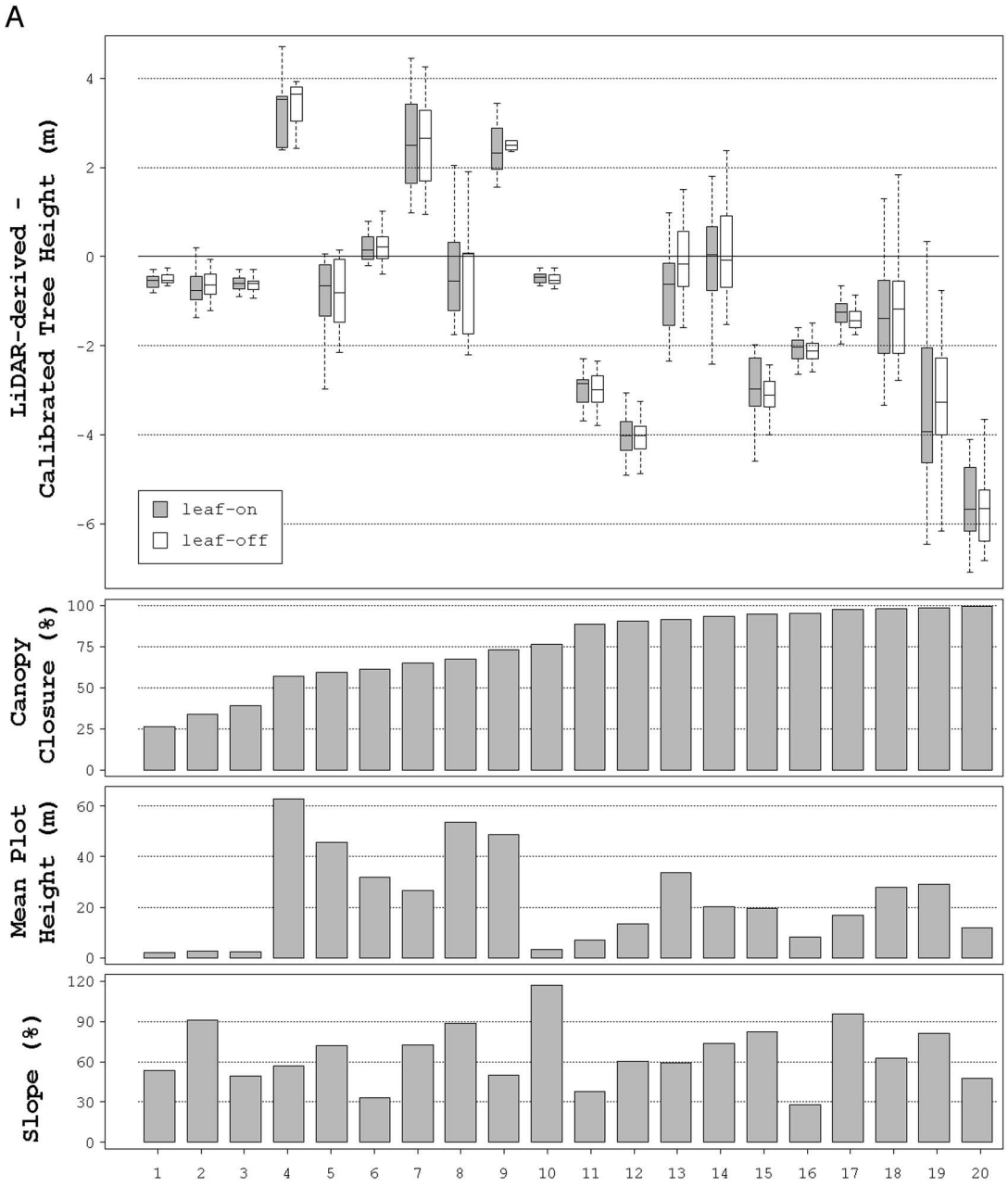

Figure 7. Distribution of error in LiDAR-assessed tree height for leaf-on and leaf-off laser data acquisitions and corresponding mean local vegetation (canopy cover and tree height) and topographic (slope) conditions across (A) coniferous, (B) mixed, and (C) hardwood vegetation plots. Boxplot whiskers indicate the range and bars the median of tree height error per plot.

stronger ($R^2 = 0.41$) for mixed vegetation plots, and all regressions were significant at $\alpha = 0.05$ (Table 4). $\bar{H}$ correlated positively to $\bar{E}_H$ across forest types, but the association, although significant at $\alpha = 0.05$, was weak ($R^2 < 0.10$). The coefficient of determination increased to 0.30 when coniferous plots only were considered. A similar relationship between plot $\bar{E}_H$, $\bar{H}$, and canopy cover was observed for leaf-off conditions, except that canopy cover was not significantly related to $\bar{E}_H$ (Table 4).

Discussion

The significance of our findings for laser-assisted forest inventory operations can perhaps be better realized when laser-derived tree height is combined with ancillary and field inventory data to assess forest productivity. Estimates of site index obtained by using stand boundary delineations and stand age data, LiDAR-derived tree heights, and the FIA site index formulas for the 42 plots with mean tree height >3 m would have assigned 12 plots at leaf-on and 11 plots at leaf-off conditions to a different (and probably wrong) productivity class compared with the one assigned by using the calibrated tree heights. Note that the range of site productivity in the study area is narrow, as practically all forestland belongs to the top two classes (in a five-class system). If we were to assume that the 45 plots were a random sample of the forests in the 9,500-ha study area, the total wood volume error calculated by using field-determined

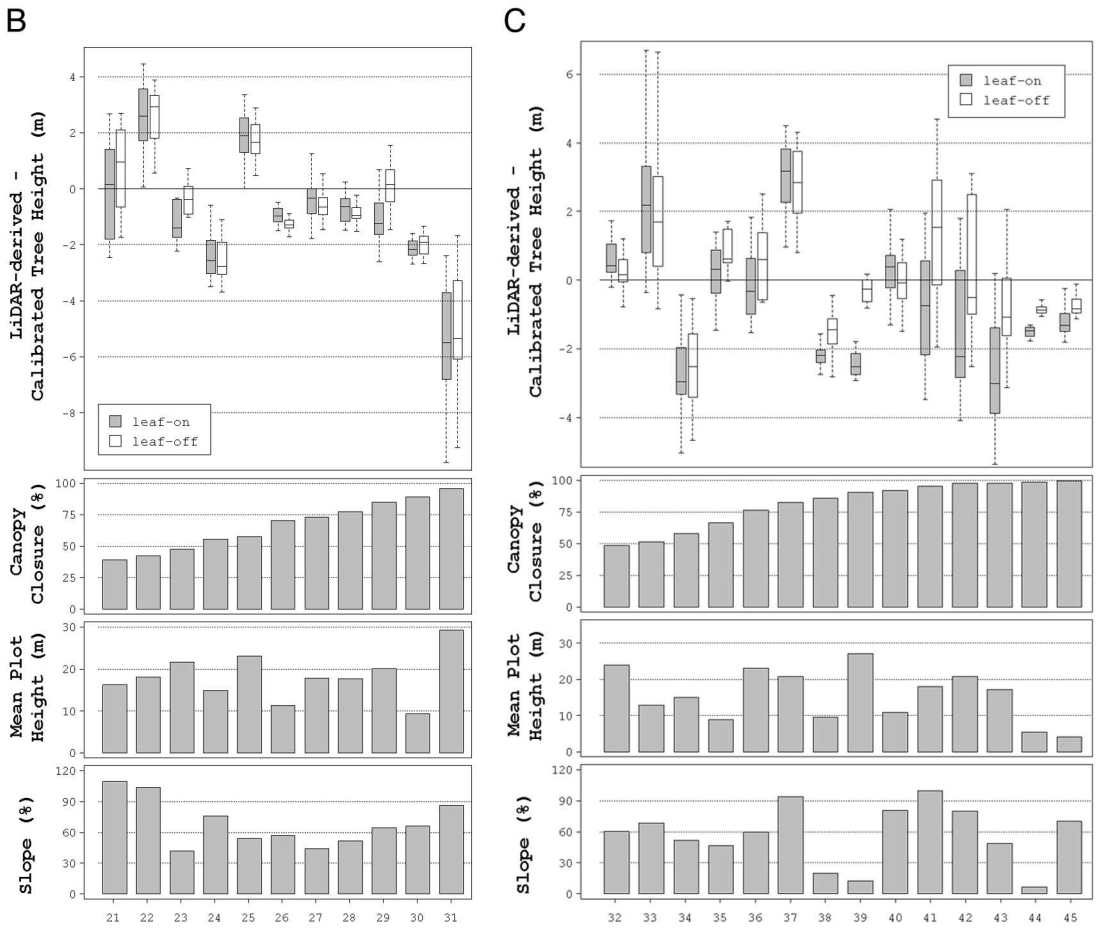

Figure 7. Continued

species and dbh data, leaf-on laser tree heights versus calibrated heights, and volume equations used by FIA (Brackett 1977, Pillsbury and Kirkley 1984) would be 480,000 m^3 (436,000 m^3 for Douglas fir and 34,000 m^3 for hardwoods). At leaf-off conditions the error for hardwoods would be 13,000 m^3. At the stand level, the absolute volume error would range from −225 to 44 m^3/ha (−42 to 9%) for conifers, −71 to 43 m^3/ha (−30 to 18%) for hardwoods using leaf-on laser data, and −42 to 39 m^3/ha (−17 to 16%) for hardwoods using leaf-off data. A volume estimation error of this magnitude is much greater than would be expected using traditional stand examinations in typical temperate rainforest conditions in the Pacific Northwest. Considering that biomass and carbon storage estimation is typically derived from volume estimates, we expect estimation error rate propagation for the former comparable to those observed in this study for volume.

Predicting the magnitude of LiDAR estimated tree height error proved very difficult. The many factors that control the formation of tree stems and crowns (phototropism, response to mechanical forces, direction of prevailing winds, species-specific genetic tendencies, and competition between adjacent trees) often lead to variability in the direction and magnitude of tree lean and complicate efforts to predict E_L. The magnitude of error in laser-based estimates of height for individual trees is potentially much higher than that in mean height estimates assessed at the plot, stand, or management unit level. Although most trees were found to lean downhill, many otherwise similar plots had trees that leaned uphill or not at all. This variability minimized the predictive power of models linking tree-lean to laser-derived vegetation and terrain parameters. Estimation of tree lean is a standard component of most forest inventory field data collection protocols, including that of FIA, and it is based on visual assessment of the horizontal displacement between the observed tree top and base. Determining the location of the tree stem and base from laser data is a challenging task, because few if any returns represent the tree stem in most forest conditions and types. Novel analytic approaches that accomplish this task and thus enable the assessment of E_L could improve the accuracy of height estimation from LiDAR data. The improvement would be substantial on steep slopes, considering that a 20-m-tall tree with an uphill leaning angle of 8° (the average leaning of trees taller than 3 m in all plots) growing on a 60% slope (the average over all plots) would incur an 8% underestimation of its true height, whereas the height of the same tree on flat land will be underestimated by a mere 1%. Further work is needed to investigate approaches with a potential to quantify tree lean.

The large DTM errors reported for many of the plots established in this study suggest that applying standardized discretization procedures in situations with comparatively low pulse energy and dense canopies can produce laser return clouds with unconventional characteristics. Analysis of return clouds for several plots indicated unusually low

rates of penetration-to-the-ground and an unusually high percentage of below-ground returns. For the plots with the largest observed DTM errors, <1% of the returns were within 0.5 m from the surveyed surface and as many as 8% of all returns were below ground. These rates depart markedly from those implicitly required or anticipated by commonly used filtering and surface generating algorithms. Given that return clouds for many plots offer almost no clues as to ground location, it is not surprising that for all plots for which mean DTM was overestimated by at least 3 m, all four human interpreters opined that it was not possible to draw a surface across return cloud transects because of inadequate reference information. Considering that human-performed filtering of returns is widely regarded as the "gold standard" (e.g., Kobler et al. 2007), errors in DTMs generated using algorithmic approaches for these plots should have been expected.

It is well established (e.g., Hyyppä et al. 2004) that all LiDAR data sets contain at least a few returns positioned below ground. Where the density of ground returns permits a detailed and accurate representation of the ground, the usual case in most acquisitions, the identification of below-ground points is reliably and easily accomplished during trial and error-based data preprocessing. In the studies reported by Chen et al. (2007) and Kobler et al. (2007), experimentation yielded positional criteria that, when implemented, eliminated all below-ground returns. In our study, despite ample effort, we were unable to identify any mechanisms capable of consistently identifying below-ground returns in plots with dense, continuous canopy, probably because of substantial variability in the local density and dispersion rates of these returns. Below-ground returns maintained in the return clouds processed by each of the three software packages used in this study are probably responsible for the elevation bias observed for many plots. The generally superior accuracy of the TerraScan-derived DTMs compared with those obtained with TreeVis and TIFFs may be a result of greater effort invested in local tuning of the algorithmic parameters used by TerraScan during DTM generation.

Laser returns coinciding with a 1-m-wide, 50-m-long transect surveyed under a dense, closed canopy of 15- to 20-m-tall Douglas fir trees (Figure 8) vividly illustrate the challenges in return filtering and the causes of DTM error. This transect starts on a landing covered with short grass and sparse brush for which the elevation of the surveyed and LiDAR DTM correspond well. However, the two DTMs diverge sharply where the transect intersects the boundary of a dense stand. Ten meters farther along they become virtually parallel, with the LiDAR-derived DTM perched 9 m above the surveyed one. At 37 m, a sharp slope inflection in the LiDAR-derived surface (that does not track any slope change in the surveyed surface) leads to even greater divergence as the transect progresses. In this area, the proportion of returns decreases rapidly with canopy depth and only a small percentage are identified at the lower half of the canopy. Ten returns positioned above the surveyed surface were eliminated during data preprocessing that used filtering criteria considered optimal and obtained by experimentation. Additional returns positioned below the surveyed surface were also eliminated. We observed similar

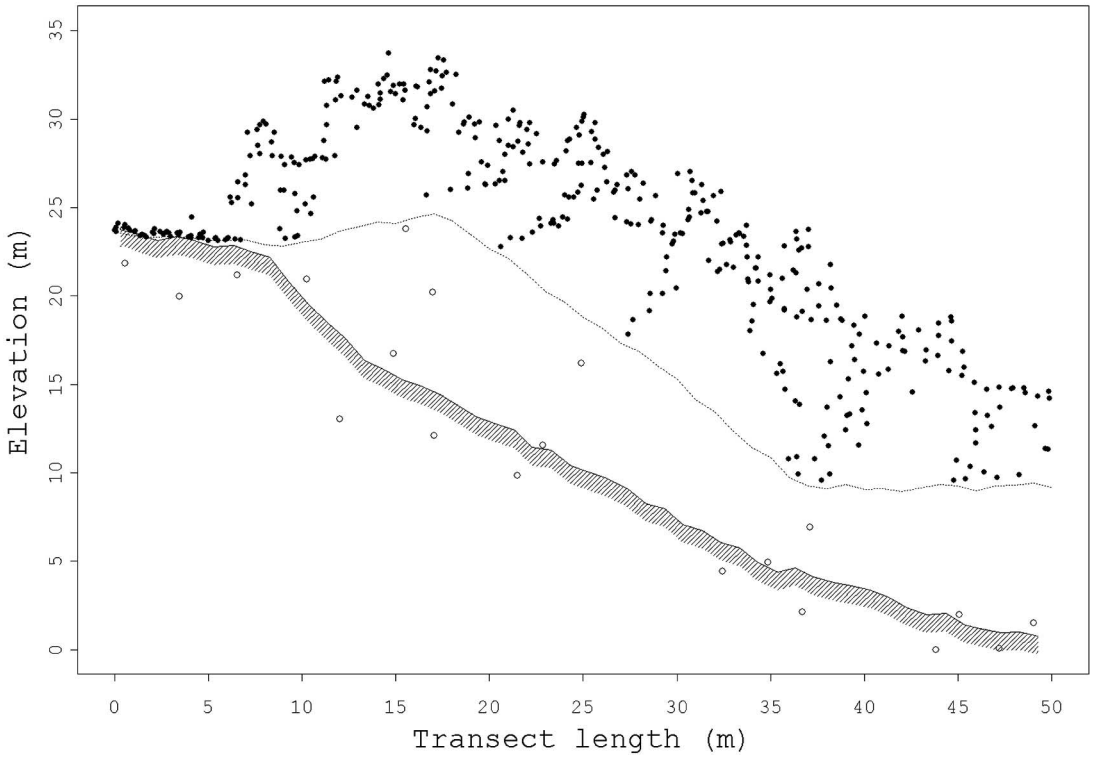

Figure 8. Spatial distribution of laser returns along a 50 by 1-m transect, retained (●) or eliminated (○) during laser data preprocessing. Lines represent the laser-derived terrain model (dotted) and the surveyed ground surface (hatch-marked, solid). Omitted are 22 more returns, located 5 m or more below the surveyed surface.

patterns of divergence on two other surveyed transects in riparian hardwood vegetation.

In low-density stands, there appears to be sufficient space between crowns for pulses to reach the ground except where dense understory vegetation poses an additional barrier. In stands characterized by uniform and many-meter-thick live foliage, typical of unthinned coniferous plantations such as the one depicted in Figure 8, very few pulses reach the ground with enough energy to be ultimately backscattered to the sensor. The overestimation of ground elevation in continuous canopy stands can sometimes be reduced or even eliminated by the presence of small openings or areas of sparse canopy. The improved pulse penetration in such locations allows formation of ground returns that guide the classification of returns as on-ground or aboveground, and, in turn, contribute to extraction of DTMs free of serious errors. All four high-canopy-cover hardwood plots with leaf-on DTM error of 1 m or less had small canopy breaks. Where slopes are steep, the improvement in DTM accuracy conferred by small openings or areas of sparse canopy tends to diminish quickly with distance from these features.

Indirect evaluations of algorithmic performance obtained by visual comparison of laser-derived and surveyed DTMs suggest that there is a tendency in all three algorithms tested to label as ground those returns that appear aligned, with some tolerance for deviations, on a plane parallel to the canopy surface. This tendency is particularly pronounced in portions of dense stands growing on steep terrain and adjacent to roads or other sizable canopy openings. It has been observed to persist in other laser data sets acquired elsewhere in western Oregon with laser instruments different from those used in this study. Algorithmic enhancements adaptive to steep terrain and low density of ground returns will probably improve the accuracy of DTMs and, therefore, tree height for some plots. Still, there will be cases where returns near the actual ground surface are too few to permit accurate terrain descriptions, at least with the kind of laser instrument and acquisition specifications used in this study.

DTM elevation overestimation linked to underestimation of laser-derived tree height can also be an artifact of reduced pulse energy. Modern, high-frequency LiDAR systems can generate high-density laser data more economically than their predecessors by operating onboard aircraft that fly higher and faster. However, because the increase in system frequency has not been matched by a comparable increase in energy, each pulse from a high-frequency system carries less energy and most or all of this energy becomes dissipated by the upper canopy layers (Chasmer et al. 2006). At 71 kHz, the repetition frequency used by the Optech 3100 instrument in this study, the average energy carried by a single pulse is 83 μJ, an amount that nearly doubles (164 μJ) when the instrument is operated at 33 kHz, the lowest frequency setting available. The larger number of pulses increases the probability that one will propagate through a small canopy opening or sparse/thin area of the canopy to the ground and thus compensate for the weaker energy carried by each pulse. In most forests, pulse density and laser instrument scanning frequency choices may be of secondary importance for the accuracy of tree height assessment, but they can be critical in temperate or tropical rainforests and where canopy cover limits pulse penetration. In the latter case, it might be prudent to consider using a lower-frequency, higher-pulse-energy system along with a high-frequency laser system. The new multiple pulses in the air (MPiA) LiDAR technology, which permits a second pulse to be emitted before the backscattering of the first is received, may offer a cost-effective solution to the frequency selection dilemma. Compared with single pulse in the air (SPiA) LiDAR instruments, MPiA enables acquisitions that maintain the same return density as SPiA with use of lower-frequency, higher-energy pulses.

Because high-pulse density, narrow-beam divergence LiDAR virtually saturates the canopy, it is unlikely that tree tops are missed. Discrepancies between the assessed and true horizontal location of tree tops rarely exceed the pulse's footprint diameter with the possible exception of flat-topped crowns. The negative bias in the elevation of identified tree tops we documented in the calibration procedure, although variable among trees (especially hardwoods at leaf-off conditions, as in Figure 4), can be estimated reliably (5- to 10-cm estimation SE) at the plot or stand level and subsequently used to correct tree top elevation. However, it would be unwise to apply such corrections to laser data acquired with lower pulse spacing, different pulse footprints, or instruments emitting different amounts of energy per pulse as this could lead to systematic bias in tree height estimates. The optimal bias correction may also be affected by the choice of discretization algorithm. The tree top elevation bias of highest returns extracted by using algorithms that focus on the "leading-edge" (or "front-end") of the pulse would probably differ from the elevation bias of returns extracted using "generic" or with "trailing-edge" ("back-end")-focusing algorithms. These terms describe discretization algorithms that generate returns at the first and last instance in which backscattered energy exceeds designated thresholds. In generic algorithms, all local backscattered energy maxima along the pulse trajectory are return candidates. Because backscattering from the tip of a conifer leader or hardwood leaf (or twig) at the top of the crown is much fainter than backscattering originating from other upper crown parts, generic algorithms fail to identify the very top of the crown, thereby causing tree top underestimation. Processing selected data subsets with both leading-edge and generic algorithms could provide estimates on the magnitude of E_T for cover types and crown forms present in an area of interest.

Considering the unpredictable variation in the direction of tree lean and the nearly constant negative bias in the estimation of tree top elevation, it is not surprising that canopy cover, the only vegetation structure parameter found to correlate consistently to E_{DTM}, was also the only parameter that correlated to E_H. Despite the significance of the relationship between canopy cover and E_H, the predictive power of regression models linking them is limited, except when subsets of plots that comply with selected vegetation characteristics identified during field visits are used to build the regression models (Table 4). These models, along with those shown in Figure 6, have been included to illustrate the

dynamics that govern the assessment of tree height from LiDAR data, not to quantify the assessment's error budget.

Leaf-off acquisitions are often advocated as the antidote to inadequate penetration by laser pulses for hardwood stands. However, we found that despite the improved DTM accuracy at leaf-off conditions for hardwood plots, the improvement in plot estimates of tree height was marginal: for only one hardwood and one mixed plot did the estimate of mean height shift from the >10% of mean height error class to the <10% class (Table 3), mainly because the error due to tree lean, although potentially minimal and little noticed in studies conducted on flat or gentle terrain, can be substantial in high-relief landscapes such as the one used for this study. The result that on nearly 4 in every 10 plots across forest types, LiDAR-derived mean height was >10% different from actual height fails to support often-repeated assertions on the precision and accuracy of tree height estimates derived from high-density LiDAR data.

Our experience from this study suggests that delivery of incomplete LiDAR data sets (in which returns have been filtered) should be avoided. The only possible gain from such a practice is a small reduction in data storage requirements. Unfiltered returns can be valuable in comparing DTM generation options and for return percentile and voxel-based attribute estimation approaches. LiDAR-based assessment of vegetation change based on acquisitions separated by many years often entails reprocessing of each laser data set. Filtering performed at the time of the first acquisition may be suboptimal at the time of the second acquisition, considering the rate of evolution in LiDAR theory and data-processing techniques. Maintaining the unfiltered data guarantees that analytical tools developed after the acquisition could still be applied to older data sets.

Conclusions

Interest in assessing forest inventory parameters via LiDAR technologies has grown tremendously over the past few years, in part as a result of reports documenting the ability of laser data to quantify the vertical profile of forest stands and accurately estimate tree height. However, most of the findings involving LiDAR-derived estimates of tree height were based on sites with topographic and vegetation conditions that are very different and arguably more favorable than those encountered in many regions of the world, including the steep and densely stocked forests of the US Pacific Northwest. Using precise, survey-grade field data and leaf-on and leaf-off LiDAR data from a study area in the temperate rainforest of the Coast Range of Oregon, we evaluated the accuracy and precision of laser-derived estimates of tree height. Results indicate that where LiDAR penetration is poor due to continuous canopies, substantial overestimation of ground elevation, confounded with tree lean, an attribute that nearly defies prediction, results in substantial error in tree height estimates. A major obstacle in the LiDAR-based assessment of tree height is the generation of accurate digital terrain models. Experimentation with different algorithms that process the laser data to identify ground returns and subsequently generate the terrain models used in the assessment of tree height suggests that although trial and error-based adjustment of algorithmic components have yielded accurate DTMs elsewhere, such efforts often fail in forest and terrain conditions prevalent in the temperate rainforests present in our study area. Optimizing the laser data acquisition specifications to ensure maximum pulse penetration to the ground or selecting leaf-off acquisition timing for hardwood or mixed forests would probably improve DTM and ultimately tree height estimation accuracy. LiDAR data discretization with both leading-edge and generic algorithms offers hope for improving estimates of tree height by quantifying tree top underestimation. Of the forest structure parameters that can be assessed via LiDAR, only canopy cover was found to be correlated (weakly) to height error. To estimate laser-derived heights in temperate rainforests growing on steep slopes with an accuracy and precision comparable to what is attainable in more conducive vegetation and terrain, techniques would need to be developed to assess tree lean, and specifications for operating the laser instrument would need to be modified with the aim of improving canopy penetration rates.

Literature Cited

ALDRED, A.H., AND J.K. HALL. 1975. Application of large-scale photography to a forest inventory. *For. Chron.* 51(1):7 p.

ANDERSEN, H.E., R.J. MCGAUGHEY, AND S.E. REUTEBUCH. 2005. Estimating canopy fuel parameters using airborne LIDAR data. *Rem. Sens. Environ.* 94:441–449.

ANDERSEN, H.E., S.E. REUTEBUCH., AND R.J. MCGAUGHEY. 2006. Rigorous assessment of tree height measurements obtained using airborne lidar and conventional field methods. *Can. J. Rem. Sens.* 32(5):355–366.

AXELSSON, P.E. 1999. Processing of laser scanner data—Algorithms and applications. *Photogramm. Rem. Sens.* 54(2–3):138–147.

BALTSAVIAS, E.P. 1999. A comparison of between photogrammetry and laser scanning. *Photogramm. Rem. Sens.* 54:83–94.

BRACKETT, M. 1977. *Notes on TARIF tree-volume computation.* DNR Report 24. State of Washington, Department of Natural Resources, Olympia, WA. 132 p.

BRANDTBERG, T., T.A. WARNER, R.E. LANDENBERGER, AND J.B. MCGRAW. 2003. Detection and analysis of individual leaf-off tree crowns in small footprint, high sampling density lidar data from the eastern deciduous forest in North America. *Rem. Sens. Environ.* 85(3):290–303.

CHASMER, L., C. HOPKINSON, B. SMITH, AND P. TREITZ. 2006. Examining the influence of changing laser pulse repetition frequencies on conifer forest canopy returns. *Photogramm. Eng. Rem. Sens.* 72(12):1359–1367.

CHEN, Q. 2007. Airborne lidar data processing and information extraction. *Photogramm. Eng. Rem. Sens.* 73(2):109–112.

CHEN, Q., P. GONG, D.D. BALDOCCHI, AND G. XIE. 2007. Filtering airborne laser scanning with morphological methods. *Photogramm. Eng. Rem. Sens.* 73(2):171–181.

CLARK, M.L., D.B. CLARK, AND D.A. ROBERTS. 2004. Small-footprint lidar estimation of sub-canopy elevation and tree height in a tropical rain forest landscape. *Rem. Sens. Environ.* 91:68–89.

ELMQVIST, M., E. JUNGERT, F. LANTZ, Å. PERSSON, AND U. SÖDERMAN. 2001. Terrain modelling and analysis using laser scanner data. *Int. Arch. Photogramm. Rem. Sens.* 34-3/W 4:219–227.

GAVEAU, D., AND R. HILL. 2003. Quantifying canopy height underestimation by laser pulse penetration in small-footprint

airborne laser scanning data. *Can. J. Rem. Sens.* 29:650–657.

GOOVAERTS, P. 1997. *Geostatistics for natural resources evaluation.* Oxford University Press, New York, NY. 483 p.

HARALICK, R.M., S.R. STERNBERG, AND X. ZHUANG. 1987. Image analysis using mathematical morphology. *IEEE Trans. Pattern Anal. Mach. Intell*. PMI-9:523–550.

HINSLEY, S.A., R.A. HILL, P.E. BELLAMY, AND H. BALTZER. 2006. The application of LiDAR in woodland bird ecology: climate, canopy structure and habitat quality, *Photogramm. Eng. Rem. Sens.* 72:1399–1406.

HODGSON, M.E., J.R. JENSEN, L. SCHMIDT, S. SCHILL, AND B. DAVIS. 2003. An evaluation of LIDAR- and IFSAR-derived digital elevation models in leaf-on conditions with USGS Level 1 and Level 2 DEMs. *Rem. Sens. Environ.* 84:295–308.

HYYPPÄ, J., H. HYYPPÄ, P. LITKEY, X. YU, H. HAGGRÉN, P. RÖNNHOLM, U. PYYSALO, J. PITKÄNEN, AND M. MALTAMO. 2004. Algorithms and methods of airborne laser scanning for forest measurements. P. 82–89 in *Proc. of the ISPRS laser-scanners for forest and landscape assessment*, Thies, M., B. Koch, H. Spiecker, and H. Weinacker (eds.). Albert Ludwigs University, Freiburg, Germany.

HYYPPÄ, J., H. HYYPPÄ, M. MALTAMO, X. YU, E. AHOKAS, AND U. PYYSALO. 2003. Laser scanning of forest resources—Some of the Finnish Experience. P. 53–59 in *Proc. of the ScanLaser scientific workshop on airborne laser scanning of forests*, September 3–4, Umeå, Sweden.

HYYPPÄ, J., U. PYYSALO, H. HYYPPÄ, AND A. SAMBERG. 2000. Elevation accuracy of laser scanning-derived digital terrain and target models in forest environment. P. 139–147 in *Proc. of the EARSel-SIG-workshop on LIDAR*, June 16–17, 2000, Dresden/FRG.

JOHNSON, E.W. 1958. The effect of photographic scale on precision of individual tree-height measurement. *Photogramm. Eng.* 24(1):142–152.

KOBLER, A., N. PFEIFER, P. OGRINC, L. TODOROVSKI, K. OŠTIR, AND S. DŽEROSKI. 2007. Repetitive interpolation: A robust algorithm for DTM generation from aerial laser scanner data in forested terrain. *Rem. Sens. Envir.* 109:9–23.

KOVATS, M. 1997. A large-scale aerial photographic technique for measuring tree heights on long-term forest installations. *Photogramm. Eng. Rem. Sens.* 63(6):741–747.

KRAUS, K., AND N. PFEIFER. 1998. Determination of terrain models in wooded areas with airborne laser scanner data. *Photogramm. Rem. Sens.* 53:193–203.

LEFSKY, M., W. COHEN, G. PARKER, AND D. HARDING. 2002. Lidar remote sensing for ecosystem studies. *Bioscience* 52:19–30.

LIM, K., P. TREITZ, M. WULDER, B. ST-ONGE, AND M. FLOOD. 2003. LiDAR remote sensing of forest structure. *Progr. Phys. Geogr.* 27(1):88–106.

LOHMANN, P., A. KOCH, AND M. SCHAEFFER. 2000. Approaches to the filtering of laser scanner data. *Int. Arch. Photogram. Rem. Sens.* 33-B3/1:534–541.

MALTAMO, M., K. MUSTONEN, J. HYYPPÄ, J. PITKANEN, AND X. YU. 2004. The accuracy of estimating individual tree variables with airborne laser scanning in a boreal nature reserve. *Can. J. For. Res.* 34:1491–1801.

MCCOMBS, J.W., S.D. ROBERTS, AND D.L. EVANS. 2003. Influence of fusing Lidar and multispectral imagery on remotely sensed estimates of stand density and mean tree height in a managed Loblolly Pine plantation. *For. Sci.* 49(3):457–466.

MCGAUGHEY, R.J. 2009. *FUSION/LDV: Software for LIDAR data analysis and visualization*. Available online at forsys.cfr.washington.edu/fusion/fusionlatest.html; last accessed Oct. 27, 2009.

MEANS, J., S. ACKER, B. FITT, M. RENSLOW, L. EMERSON, AND C. HENDRIX. 2000. Predicting forest stand characteristics with airborne scanning LIDAR. *Photogramm. Eng. Rem. Sens.* 66:1367–1371.

NAESSET, E. 1997. Determination of mean tree height of forest stands using an airborne laser scanner data. *Photogramm. Rem. Sens.* 52:49–56.

NAESSET, E. 2002. Predicting forest stand characteristics with airborne laser using a practical two-stage procedure and field data. *Rem. Sens. Envir.* 80:88–99.

NILSSON, M., T. BRANDTBERG, O. HAGNER, J. HOLMGREN, Å. PERSSON, O. STEINVALL, H. STERNER, U. SÖDERMAN, AND H. OLSSON. 2003. Laser scanning of forest resources—The Swedish experience. P. 43–52 in *Proc. of the ScanLaser scientific workshop on airborne laser scanning of forests*, September 3–4, Umeå, Sweden.

PERSSON, A., J. HOLMGREN, AND U. SÖDERMAN. 2002. Detecting and measuring individual trees using an airborne laser scanner. *Photogramm. Eng. Rem. Sens.* 68(9):925–932.

PILLSBURY, N.H., AND M.L. KIRKLEY. 1984. *Equations for total, wood, and saw-log volume for thirteen California hardwoods.* PNW Res. Note PNW-414. Pacific Northwest Res. Stn., Portland, OR. 52 p.

POPESCU, S.C., R.H. WYNNE, AND R.F. NELSON. 2002. Estimating plot-level tree heights with lidar: local filtering with a canopy height based variable window size. *Comput. Electron. Agric.* 37:71–95.

POPESCU, S., AND K. ZHAO. 2007 A voxel-based LIDAR method for estimating crown base height for deciduous and pine trees. *Rem. Sens. Environ.* 112(3):767–781.

REUTEBUCH, S.E., R.J. MCGAUGHEY, H.E. ANDERSEN, AND W.W. CARSON. 2003. Accuracy of a high-resolution lidar terrain model under a conifer forest canopy. *Can. J. Rem. Sens.* 29(5)527–535.

SITHOLE, G. 2001. Filtering of laser altimetry data using a slope adaptive filter. *Int. Arch. Photogramm. Rem. Sens.* 34-3/W 4:203–210.

SITHOLE, G., AND G. VOSSELMAN. 2004. Experimental comparison of filter algorithms for bare-earth extraction from airborne laser scanning points clouds. *ISPRS J. Photogramm. Rem. Sens.* 59:85–101.

SOHN, G., AND I. DOWMAN. 2002. Terrain surface reconstruction by the use of tetrahedron model with the MDL criterion. *Int. Arch. Photogramm. Rem. Sens.* 34-3A:336–344.

VOSSELMAN, G. 2000. Slope based filtering of laser altimetry data. *Int. Arch. Photogram. Rem. Sens.* 33-B3/ 2:935–942.

WEINACKER, H., B. KOCH, AND R. WEINACKER. 2004. TreeVis—A software system for simultaneous 3D real time visualization of DTM, laser raw data, multispectral data, simple tree and building models. P. 95 in *Proc. of the ISPRS working group VIII/2 on "Laser-scanners for forest and landscape assessment,"* Oct. 3-, Freiburg, Germany, Vol. 90.

WULDER, M. 2003. The current status of laser scanning of forests in Canada and Australia. P. 21–33 in *Proc. of the ScanLaser* Scientific Workshop on Airborne Laser Scanning of Forests, Sept. 3–4, Umeå, Sweden.

YU, X., J. HYYPPÄ, H. KAARTINEN, AND M. MALTAMO. 2004. Automatic detection of harvested trees and determination of forest growth using airborne laser scanning. *Rem. Sens. Envir.* 90:451–462.

ZHANG, K., S. CHEN, D. WHITMAN, M. SHYU, J. YAN, AND C. ZHANG. 2003. A progressive morphological filter for removing nonground measurements from airborne LIDAR data. *IEEE Trans. Geosc. Rem. Sen.* 41(4):872–882.